FINITE ELEMENT ANALYSIS OF SHEAR-DEFORMATION AND ROTATORY INERTIA FOR BEAM VIBRATION

Ana Carolina Azevedo Vasconcelos

Anderson Soares da Costa Azevêdo

Simone dos Santos Hoefel

carol-2506@hotmail.com

anderson4r2@hotmail.com

simone.santos@ufpi.edu.br

Universidade Federal do Piauí

Campus Universitário Ministro Petrônio Portella − Bairro Ininga, CEP: 64049-550, Teresina, Piauí, Brazil

Abstract. *Vibration analysis of a beam is an important subject of study in engineering. All real physical structures, when subjected to loads or displacements, behave dynamically. In case of structure with large aspect ratio of height and length the Timoshenko beam theory (TBT) is used, instead of the Euler-Bernoulli theory (EBT), since it takes both shear and rotary inertia into account. Shear effect is extremely large in higher vibration modes due to reduced mode half wave length. In this paper, the full development and analysis of TBT for the transversely vibrating uniform beam are presented for classical boundary condition. Finally, a finite element is developed in terms of dimensionless parameters of rotatory and shear. The stiffness and mass matrices for a two-node beam element with two degree of freedom per node is obtained based upon Hamilton's principle. Cubic and quadratic Lagrangian polynomials are made interdependent by requiring them to satisfy both of the homogeneous differential equations associated with TBT. Numerical examples are given for some boundary conditions. The results showed that for frequencies above critical frequency, Timoshenko beams presents distinct mode shapes behavior including the presence of double eigenvalues, shear mode or remarkably modes.*

Keywords: *Finite element method, Timoshenko, Critical frequency*

1 INTRODUCTION

Although the classical Euler-Bernoulli theory predicts the frequencies of flexural vibration of lower modes of slender beams quite accurately, it becomes inaccurate at higher modes or for deep beams where the effects of transverse shear deformation and rotatory inertia become significant. Beam theory with both contribution of rotary inertia and shear deformation was initially proposed by Timoshenko (1921). The results of that formulation were more accurate for thicker beams than the theories developed previously by Euler and Bousquet (1744) and Rayleigh (1877).

Traill-Nash and Collar (1953) found the governing equation of dynamic motion for Timoshenko beams and the frequency equations for some boundary conditions. In their research, they observed the presence of a new spectre of frequency for free-free and hinged-hinged cases. Anderson (1953) and Dolph (1954) confirmed the results obtained by Traill-Nash and Collar (1953). In order to improve Timoshenko beam results for higher frequencies (frequencies above critical frequency), Cowper (1966) developed a general expression for shape factor based on elasticity. Thomas and Abbas (1975), Downs (1976) and Levinson and Cooke (1982) are credited for studies on the dynamic behavior of Timoshenko beams from higher frequencies. Han et al. (1999) was the first to present a wider study of beams in general by discussing the four theories (Euler-Bernoulli, Rayleigh, Shear and Timoshenko).

New numerical methods developed from the middle of the past century provide a better and more convenient tool. Among them, the method of finite elements is definitely unmatched. During the last years, different finite elements were developed to study the behavior of Timoshenko beams. They are distinguished into the choice of interpolation functions for mathematical description of beam deflection and cross-section rotation and can be divided into two classes, simple and complex. A simple element is one which, for unidirectional bending in a principal plane, has a total of four degrees of freedom, two at each of two nodes. A complex element is one with more than four degrees of freedom, having more than two degrees of freedom at a node or more than two nodes (Tessler and Dong, 1981). The first Timoshenko-type element was due to McCalley (1963), who developed a two-node four dof (degrees of freedom) element. This was extended to tapered beams by Archer (1965). Severn (1970) and Davis et al. (1972), using slightly different approaches, arrived at the same or equivalent results as McCalley (1963). The commonality among these formulations is that they begin with a displacement characterization as the sum of a bending deflection and shear deflection. By means of a statical moment-shear equilibrium condition, these two deflections can be combined into one. In this connection, mention is made of a similar procedure used by Egle (1969) to arrive at an approximate version of Timoshenko beam theory that was employed by others in their beam element formulations.

Beam elements based on variational principle include those by Carnegie et al. (1969) and Dong and Secor (1973). A highly attractive feature with this approach is that only C_O continuity of v and θ is required for full interelement continuity. Here the distribution of the two kinematic variables that describe the beam translation and rotation are assumed using Lagrangian interpolation functions. Nickell and Secor (1972) and Thomas et al. (1973) tried different order polynomials for the two different variables, where again the order of one of the polynomials was larger than required. All of these elements gave reasonable results for short thick beams, but produced overly stiff results (commonly known as shear-locking) for long slender beams.

Hughes et al. (1977) was the first to develop a low-order two-node element based upon

CILAMCE 2016

Proceedings of the *XXXVII Iberian Latin-American Congress on Computational Methods in Engineering*
Suzana Moreira Ávila (Editor), ABMEC, Brasília DF, Brazil, November 6-9, 2016

linear polynomials (two dof/node) for each of the variables. This element, which was formulated using selective reduced integration, produced reasonably accurate results over a broad range of beam thickness/length ratios (i.e., free of shear-locking). Tessler and Dong (1981) use a polynomial for the translational displacement v that is one-order higher than the rotational displacement θ and then impose a constraint that makes the two polynomials interdependent. The imposed constraint is equivalent to requiring the displacements to satisfy one of the partial differential equations associated with the homogeneous form of Timoshenko beam theory. Friedman and Kosmatka (1993) extended the approach of Tessler and Dong (1981) to include two constraints using a cubic and quadratic Lagrangian polynomials for the transverse and rotational displacements, respectively, where the polynomials are made interdependent by requiring them to satisfy both of the homogeneous differential equations associated with Timoshenko beam theory.

In this paper, the motions equation are derived from Euler-Lagrange equation. The effects of transverse shear deformation and rotatory inertia are included in the governing equations. The stiffness and mass matrices for a two-node beam element with two dof/ node is obtained based upon Hamilton's principle. Cubic and quadratic Lagrangian polynomials are made interdependent by requiring them to satisfy both of the homogeneous differential equations associated with TBT. Mode shapes and frequencies curves were determined for some boundary conditions in order to investigate Timoshenko beam behavior for higher frequencies. The results obtained by Finite Element Method (FEM) are discussed and compared with analytical solutions.

2 TIMOSHENKO BEAM MODEL

Timoshenko (1921) proposed a beam model which includes both rotatory inertia and shear deformation effects to classical theory. Timoshenko theory is a major improvement for non-slender beams and for high-frequency responses where shear or rotary effects are not negligible. The potential energy of the beam is derived partly from the bending deformation and partly from the shear deformation. Therefore, total potential energy is given by:

$$U = \frac{1}{2}\int_0^L EI\left(\frac{\partial \psi(x,t)}{\partial x}\right)^2 dx + \frac{1}{2}\int_0^L \kappa GA\left(\psi(x,t) - \frac{\partial v(x,t)}{\partial x}\right)^2 dx, \tag{1}$$

where L is the length of beam, A, the cross-sectional area, I, the moment of inertia of cross section, E, the modulus of elasticity, G the modulus of rigidity, κ is the shape factor or shear coefficient, $v(x,t)$ is the transverse deflection and $\psi(x,t)$ is the total slope at the axial location x and time t.

The kinetic energy of the beam is derived partly from the motion of translation and partly from the rotation and is given by:

$$T = \frac{1}{2}\int_0^L \rho A\left(\frac{\partial v(x,t)}{\partial t}\right)^2 dx + \frac{1}{2}\int_0^L \rho I\left(\frac{\partial \psi(x,t)}{\partial t}\right)^2 dx, \tag{2}$$

where ρ is the mass per unit volume. Equation of motion is obtained using Hamilton's principle:

$$\int_{t_1}^{t_2} \delta(T-U)dt + \int_{t_1}^{t_2} \delta W_{nc}dt = 0, \tag{3}$$

where δW_{nc} is the virtual work done by non conservative forces, t_1 and t_2 are times at which the configuration of the system is known and $\delta(\ )$ is the symbol denoting virtual change, in the quantity in parentheses. Substituting Eq. (1) and Eq. (2) on the Eq. (3) and, after some manipulations, we have two coupled equations expressed as:

$$\rho A \frac{\partial^2 v(x,t)}{\partial t^2} + \kappa G A \left(\frac{\partial \psi(x,t)}{\partial x} - \frac{\partial^2 v(x,t)}{\partial x^2} \right) = 0, \tag{4}$$

$$\kappa G A \left(\psi(x,t) - \frac{\partial v(x,t)}{\partial x} \right) - EI \frac{\partial^2 \psi(x,t)}{\partial x^2} + \rho I \frac{\partial^2 \psi(x,t)}{\partial t^2} = 0. \tag{5}$$

Equations (4) and (5) can be expressed as two decoupled equations:

$$EI \frac{\partial^4 v(x,t)}{\partial x^4} + \rho A \frac{\partial^2 v(x,t)}{\partial t^2} - \frac{\rho EI}{\kappa G} \frac{\partial^4 v(x,t)}{\partial t^2 \partial x^2} - \rho I \frac{\partial^4 v(x,t)}{\partial x^2 \partial t^2} + \frac{\rho^2 I}{\kappa G} \frac{\partial^4 v(x,t)}{\partial t^4} = 0, \tag{6}$$

$$EI \frac{\partial^4 \psi(x,t)}{\partial x^4} + \rho A \frac{\partial^2 \psi(x,t)}{\partial t^2} - \frac{\rho EI}{\kappa G} \frac{\partial^4 \psi(x,t)}{\partial t^2 \partial x^2} - \rho I \frac{\partial^4 \psi(x,t)}{\partial x^2 \partial t^2} + \frac{\rho^2 I}{\kappa G} \frac{\partial^4 \psi(x,t)}{\partial t^4} = 0. \tag{7}$$

Assume that the beam is excited harmonically with an angular frequency ω and

$$v(x,t) = V(x)e^{jft}, \quad \psi(x,t) = \Psi(x)e^{jft},$$

$$\xi = x/L, \quad b^2 = \frac{\rho A L^4}{EI} \omega^2, \quad \text{with} \quad \omega = 2\pi f, \tag{8}$$

where $j = \sqrt{-1}$, ξ is the non-dimensional length of the beam, f is the natural frequency and $V(x)$ and $\Psi(x)$ are the normal functions of $v(x)$ and $\psi(x)$ respectively. Substituting the relations presented in Eq. (8) into Eqs. (6 - 7) and omitting the common term e^{jft} we obtain:

$$\frac{\partial^4 V(\xi)}{\partial \xi^4} + b^2 s^2 \frac{\partial^2 V(\xi)}{\partial \xi^2} + b^2 r^2 \frac{\partial^2 V(\xi)}{\partial \xi^2} + b^4 r^2 s^2 V(\xi) - b^2 V(\xi) = 0, \tag{9}$$

$$\frac{\partial^4 \Psi(\xi)}{\partial \xi^4} + b^2 s^2 \frac{\partial^2 \Psi(\xi)}{\partial \xi^2} + b^2 r^2 \frac{\partial^2 \Psi(\xi)}{\partial \xi^2} + b^4 r^2 s^2 \Psi(\xi) - b^2 \Psi(\xi) = 0, \tag{10}$$

where r and s are coefficients related with the effect of rotatory inertia and shear deformation given by:

$$r^2 = \frac{I}{AL^2} \quad \text{and} \quad s^2 = \frac{EI}{\kappa AGL^2}, \tag{11}$$

We must consider two cases when obtaining Timoshenko beam model spatial solution. In the first case, assume:

$$\sqrt{(r^2 - s^2)^2 + 4/b^2} > (r^2 + s^2) \quad \text{which leads to} \quad b < \frac{1}{(r\,s)}, \tag{12}$$

while in the second

$$\sqrt{(r^2 - s^2)^2 + 4/b^2} < (r^2 + s^2) \quad \text{which leads to} \quad b > \frac{1}{(r\,s)}. \tag{13}$$

Substituting $b = 1/(rs)$ in b relation presented on Eq. (8), we have the critical frequency expressed as:

$$\omega_{crit} = \sqrt{\frac{\kappa G A}{\rho I}} \quad \text{or} \quad f_{crit} = \frac{\sqrt{\kappa G A/\rho I}}{2\pi}. \tag{14}$$

We call this cutoff value $b_{crit} = 1/(rs)$. When $b < b_{crit}$ the solution of Eqs. (6) and (7) can be expressed respectively, in trigonometric and hyperbolic functions:

$$V(\xi) = C_1 cosh(\alpha_{t1}\xi) + C_2 sinh(\alpha_{t1}\xi) + C_3 cos(\beta_t\xi) + C_4 sin(\beta_t\xi), \tag{15}$$
$$\Psi(\xi) = C_1' sinh(\alpha_{t1}\xi) + C_2' cosh(\alpha_{t1}\xi) + C_3' sin(\beta_t\xi) + C_4' cos(\beta_t\xi), \tag{16}$$

with

$$\alpha_{t1} = \frac{b}{\sqrt{2}} \left[-(r^2 + s^2) + \sqrt{(r^2 - s^2)^2 + \frac{4}{b^2}} \right]^{1/2} \tag{17}$$

and

$$\beta_t = \frac{b}{\sqrt{2}} \left[(r^2 + s^2) + \sqrt{(r^2 - s^2)^2 + \frac{4}{b^2}} \right]^{1/2}. \tag{18}$$

Equations (15) and (16) have two eigenvalues, α_{t1} and β_t, that are related with trigonometric and hyperbolic sines and cosines, respectively. When $b > b_{crit}$ the solution $V(\xi)$ and $\Psi(\xi)$ can be expressed only in trigonometric functions:

$$V(\xi) = \overline{C}_1 cos(\alpha_{t2}\xi) + \overline{C}_2 sin(\alpha_{t2}\xi) + \overline{C}_3 cos(\beta_t\xi) + \overline{C}_4 sin(\beta_t\xi), \tag{19}$$
$$\Psi(\xi) = \overline{C}_1' sin(\alpha_{t2}\xi) + \overline{C}_2' cos(\alpha_{t2}\xi) + \overline{C}_3' sin(\beta_t\xi) + \overline{C}_4' cos(\beta_t\xi), \tag{20}$$

with

$$\alpha_{t2'} = j\frac{b}{\sqrt{2}} \left[(r^2 + s^2) - \sqrt{(r^2 - s^2)^2 + \frac{4}{b^2}} \right]^{1/2} = j\,\alpha_{t2} \tag{21}$$

and

$$\beta_t = \frac{b}{\sqrt{2}} \left[(r^2 + s^2) + \sqrt{(r^2 - s^2)^2 + \frac{4}{b^2}} \right]^{1/2}. \tag{22}$$

Notice that $\alpha_{t2'}$ values are always complex. The Equations (19) and (20) have two eigenvalues α_{t2} and β_t which leads to two pair of frequency equations for each boundary conditions. The relations between the coefficients in Eqs. (15) and (16), or Eqs. (19) and (20) can be found in Huang (1961) and Soares and Hoefel (2015).

In the literature, some researchers adopted a terminology to separate these pairs in two distinct spectra: the "first spectrum" for $b < b_{crit}$ and the "second spectrum" for $b > b_{crit}$.

Traill-Nash (1953) first claimed the existence of double eigenvalue for hinged-hinged boundary conditions for $b > b_{crit}$. They noted that modes shapes given by Eq. (15) are similar to Eq. (19). Due to this phenomena the frequencies found were separated in two distinct spectra: the first spectrum which is represented by $sin(\beta_t) = 0$ and the second spectrum which is represented by $sin(\alpha_{t2}) = 0$. However, Downs (1976) noted that mode shapes of each spectra of frequencies although similar are distinct, because deformations due to shear and deflection are of the same phase and are summed to give the total transverse deflection for $b < b_{crit}$, while for $b > b_{crit}$ the shear and bending deformation are opposed with the net transverse deflection equal to their difference as can be observed in Fig. 1.
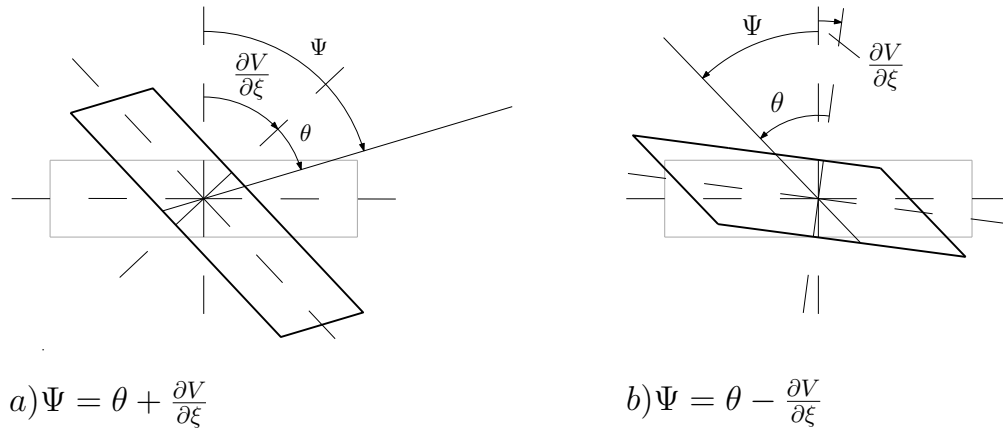

$$a)\ \Psi = \theta + \frac{\partial V}{\partial \xi} \qquad\qquad b)\ \Psi = \theta - \frac{\partial V}{\partial \xi}$$

Figure 1: Free vibration of Timoshenko beam: (a) $b < b_{crit}$ **; (b)** $b > b_{crit}$

Table 1 presents frequency equations obtained considering $b < b_{crit}$ and $b > b_{crit}$ for clamped-clamped (c-c), hinged-hinged (h-h) and sliding-sliding(s-s) Timoshenko beam.

Table 1: Frequency equations of Timoshenko model

	frequency equation ($b < b_{crit}$)
c-c	$2 - 2cosh(\alpha_{t1})cos(\beta_t) + \dfrac{b(b^2 s^2 (r^2 - s^2)^2 + (3s^2 - r^2))}{\sqrt{1 - b^2 r^2 s^2}} sinh(\alpha_{t1})sin(\beta_t) = 0$
h-h	$sin(\beta_t)sinh(\alpha_{t1}) = 0$
s-s	$\dfrac{b^2 s^2 (\alpha_{t1}^2 - \beta_t^2)(b^2 s^2 (\beta_t^2 - \alpha_{t1}^2) + 2\beta_t^2 \alpha_{t1}^2)}{\alpha_{t1}\beta_t^3 L^2} sin(\beta_t)sinh(\alpha_{t1}) = 0$

	frequency equation ($b > b_{crit}$)
c-c	$2 - 2cos(\alpha_{t2})cos(\beta_t) + \dfrac{b(b^2 s^2 (r^2 - s^2)^2 + (3s^2 - r^2))}{\sqrt{b^2 r^2 s^2 - 1}} sin(\alpha_{t2})sin(\beta_t) = 0$
h-h	$sin(\alpha_{t2})sin(\beta_t) = 0$
s-s	$\dfrac{(\beta_t^2 - \alpha_{t2}^2)s}{\alpha_{t2}\beta_t} sin(\beta_t)sin(\alpha_{t1}) = 0$

Soares and Hoefel (2015) observed that, when r and s approaches zero, TBT frequency

CILAMCE 2016

Proceedings of the *XXXVII Iberian Latin-American Congress on Computational Methods in Engineering*
Suzana Moreira Ávila (Editor), ABMEC, Brasília DF, Brazil, November 6-9, 2016

equations becomes identical to EBT frequency equation and that b_{crit} approaches infinity. It can be observed in Eq. (8) that if b_{crit} approaches infinity, f_{crit} can no longer be defined, in fact f_{crit} only appears if both rotatory inertia and shear deformation effects are considered.

The natural frequency f is written in terms of two eigenvalues (α_{t1} and β_t or α_{t2} and β_t) as follows (Huang, 1961):

$$f_i = \frac{\sqrt{\beta_t^2 - \alpha_{t1}^2}}{2\pi\sqrt{r^2 + s^2}} \left(\frac{EI}{\rho AL^4}\right)^{1/2} \quad \text{with} \quad i = 1, 2, ..., n. \quad \text{when} \quad b < b_{crit}, \tag{23}$$

$$f_i = \frac{\sqrt{\beta_t^2 + \alpha_{t2}^2}}{2\pi\sqrt{r^2 + s^2}} \left(\frac{EI}{\rho AL^4}\right)^{1/2} \quad \text{with} \quad i = 1, 2, ..., n. \quad \text{when} \quad b > b_{crit}. \tag{24}$$

3   FINITE ELEMENT FORMULATION

The element model is showed in Fig. 2, the generalized coordinates at each node are V, the total deflection, and Ψ, the total slope. This results in a element with four degrees of freedom thus enabling the expression for V and Ψ to contain two undetermined parameters each, which can be replaced by the four nodal coordinates.
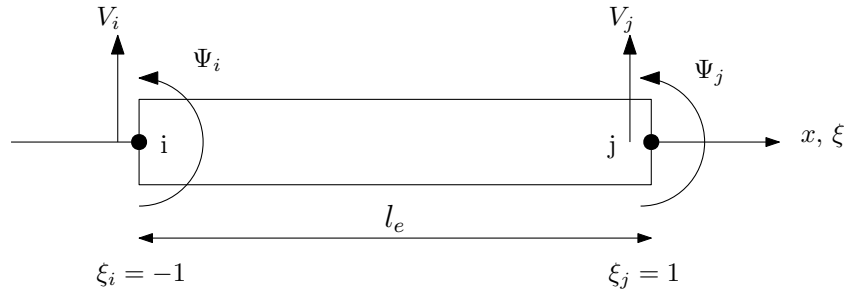

Figure 2: Beam element

Using the non-dimension coordinate (ξ) and element length l_e defined in Fig. 2, the displacement V and total slope Ψ can be written in matrix form as follows:

$$V = [\mathbf{N}(\xi)]\{\mathbf{v}\}_e \quad \text{and} \quad \Psi = [\overline{\mathbf{N}}(\xi)]\{\mathbf{v}\}_e. \tag{25}$$

where

$$[\mathbf{N}(\xi)] = [N_1(\xi) \quad N_2(\xi) \quad N_3(\xi) \quad N_4(\xi)], \tag{26}$$

$$[\overline{\mathbf{N}}(\xi)] = [\overline{N}_1(\xi) \quad \overline{N}_2(\xi) \quad \overline{N}_3(\xi) \quad \overline{N}_4(\xi)]. \tag{27}$$

In the current development, a cubic shape and a quadratic shape functions are proposed, respectively, as follows:

$$N_i(\xi) = \sum_{i=0}^{3} \lambda_i \xi^i \quad \text{and} \quad \overline{N}_i(\xi) = \sum_{i=0}^{2} \overline{\lambda}_i \xi^i, \tag{28}$$

where λ_i and $\overline{\lambda}_i$ are shape functions coefficients. These coefficients are determined by requiring shape functions N_i and $\overline{N}_i$ to exactly satisfy both homogeneous form of TBT static equations

of equilibrium:

$$\kappa GA \left(\frac{\partial \psi}{\partial x} - \frac{\partial^2 v}{\partial x^2} \right) = 0, \tag{29}$$

$$\kappa GA \left(\psi - \frac{\partial v}{\partial x} \right) - EI \frac{\partial^2 \psi}{\partial x^2} = 0. \tag{30}$$

The displacements functions in Eqs. (26) and (27) can be expressed in terms of dimensionless parameters of rotatory (r) and shear (s):

$$\mathbf{N_i}(\xi) = \frac{1}{4(3s^2 + 1)} \begin{bmatrix} 2(3s^2 + 1) - 3(2s^2 + 1)\xi + \xi^3 \\ a\left[3s^2 + 1 - \xi - (3s^2 + 1)\xi^2 + \xi^3\right] \\ 2(3s^2 + 1) + 3(2s^2 + 1)\xi - \xi^3 \\ a\left[-3s^2 - 1 - \xi + (3s^2 + 1)\xi^2 + \xi^3\right] \end{bmatrix}, \tag{31}$$

and

$$\overline{\mathbf{N}}_{\mathbf{i}}(\xi) = \frac{1}{4(3s^2 + 1)} \begin{bmatrix} a\left(3\xi^2 - 3\right) \\ -1 - 2(3s^2 + 1)\xi + 6s^2 + 3\xi^2 \\ a\left(3 - 3\xi^2\right) \\ -1 + 2(3s^2 + 1)\xi + 6s^2 + 3\xi^2 \end{bmatrix}, \tag{32}$$

where $a = l_e/2$.

Potential and Kinetic energy expressions presented in Eqs. (1) and (2) for an elemental length l_e of a uniform Timoshenko beam are given by:

$$\boldsymbol{U_e} = \frac{1}{2} \frac{EI}{a} \int_{-1}^{1} \left(\frac{\partial \Psi}{\partial \xi} \right)^2 d\xi + \frac{1}{2} \frac{EI}{a \, s^2} \int_{-1}^{1} \left(\frac{1}{a} \frac{\partial V}{\partial \xi} - \Psi \right)^2 d\xi, \tag{33}$$

$$\boldsymbol{T_e} = \frac{1}{2} \rho Aa \int_{-1}^{1} \left(\frac{\partial V}{\partial t} \right)^2 d\xi + \frac{1}{2} r^2 \rho Aa^3 \int_{-1}^{1} \left(\frac{\partial \Psi}{\partial t} \right)^2 d\xi, \tag{34}$$

where V is the deflection, Ψ and $\partial V/\partial \xi$ are the total and bending slope, respectively. Substituting the displacement expression (Eq. 25) into the potential energy (Eq. 33) gives:

$$\begin{aligned}
\boldsymbol{U_e} &= \frac{1}{2} \{\mathbf{v}\}_e^T \left[\frac{EI}{a} \int_{-1}^{1} [\overline{\mathbf{N}}(\xi)']^T [\overline{\mathbf{N}}(\xi)'] d\xi \right] \{\mathbf{v}\}_e + \\
&\quad \frac{1}{2} \{\mathbf{v}\}_e^T \left[\frac{EI}{a \, s^2} \int_{-1}^{1} [\mathbf{N}(\xi)' - \overline{\mathbf{N}}(\xi)]^T [\mathbf{N}(\xi)' - \overline{\mathbf{N}}(\xi)] d\xi \right] \{\mathbf{v}\}_e,
\end{aligned} \tag{35}$$

where $[\mathbf{N}(\xi)'] = [\partial \mathbf{N}(\xi)/\partial \xi]$. Therefore the element stiffness matrix is given by:

$$\begin{aligned}
[\boldsymbol{k_e}] &= \left[\frac{EI}{a} \int_{-1}^{1} [\overline{\mathbf{N}}(\xi)']^T [\overline{\mathbf{N}}(\xi)'] d\xi + \right. \\
&\quad \left. \frac{EI}{a \, s^2} \int_{-1}^{1} [\mathbf{N}(\xi)' - \overline{\mathbf{N}}(\xi)]^T [\mathbf{N}(\xi)' - \overline{\mathbf{N}}(\xi)] d\xi \right].
\end{aligned} \tag{36}$$

Substituting the displacement expression (Eq. 25) into the kinetic energy (Eq. 34) gives:

$$\boldsymbol{T}_e = \frac{1}{2} \{\dot{\mathbf{v}}\}_e^T \left[\rho A a \int_{-1}^{1} [\mathbf{N}(\xi)]^T [\mathbf{N}(\xi)] d\xi + r^2 \rho A a^3 \int_{-1}^{1} [\overline{\mathbf{N}}(\xi)]^T [\overline{\mathbf{N}}(\xi)] d\xi \right] \{\dot{\mathbf{v}}\}_e, \quad (37)$$

Therefore the element mass matrix is given by:

$$[\boldsymbol{m_e}] = \left[\rho A a \int_{-1}^{1} [\mathbf{N}(\xi)]^T [\mathbf{N}(\xi)] d\xi + r^2 \rho A a^3 \int_{-1}^{1} [\overline{\mathbf{N}}(\xi)]^T [\overline{\mathbf{N}}(\xi)] d\xi \right]. \quad (38)$$

4 NUMERICAL RESULTS

This section presents numerical examples for Timoshenko beams subjected to four boundary conditions: hinged-hinged, slinding-slinding , hinged-slinding and clamped-clamped. These boundary conditions are defined in Table 2. The same parameters value are considered for all examples. A beam of rectangular cross section such that $L = 0.5\,m$, $H/L = 0.25$, $\kappa = 5/6$, $E = 210\,GPa$, $G = 80.8\,GPa$ and $\rho = 7850\,kg/m^3$ are considered. The values at inertia rotary and shear deformation factors, are respectively, $r = 0.0722$ and $s = 0.1275$. This example was presented by Levison and Cooke in 1982.

Table 2: Boundary Conditions

Boundary Condition	Shear Force	Moment	Total Slope	Deflection
Hinged	-	$\dfrac{\partial \Psi(\xi)}{\partial \xi} = 0$	-	$V(\xi) = 0$
Clamped	-	-	$\Psi(\xi) = 0$	$V(\xi) = 0$
Sliding	$\Psi(\xi) - \dfrac{1}{L}\dfrac{\partial V(\xi)}{\partial \xi} = 0$	-	$\Psi(\xi) = 0$	-

4.1 Hinged-hinged beam

Considering a hinged-hinged beam, the first fourteen natural frequencies are presented in the Table 3: the first ten frequencies from the first spectrum, the first four frequencies from the second spectrum, and the shear mode frequency. The second column represents the analytical results obtained by reference adopted (Levinson and Cooke, 1982), and the third and fifth columns represent FEM results for 30 elements and 70 elements, respectively. Fourth and sixth columns show the error between analytical and FEM results. An observation that must be made is the value of shear mode frequency from second column. This value corresponds to shear mode found by Azevedo et al. (2016), since a typographic error appear to be present in Levinson and Cooke (1982), for the shear mode value, which do not appear to have been noted in the literature. Notice that for higher modes, error decreases when the number of elements is increased. Therefore, FEM formulation presents a good accuracy.

Table 3: Natural frequencies for the hinged - hinged Timoshenko beam (rad/s)

	1st Spectrum					2nd Spectrum				
Mode	TBT	FEM - 30e		FEM - 70e		Mode	TBT	FEM - 30e		FEM - 70e	
Number	Frequency	Frequency	Error (%)	Frequency	Error (%)	Number	Frequency	Frequency	Error (%)	Frequency	Error (%)
1	6712	6712.85	0.0127	6712.53	0.0078	1	89077	89420.32	0.3854	89151.54	0.0837
2	22136	22150.95	0.0675	22139.61	0.0163	2	108044	108691.89	0.5996	108174.10	0.1204
3	40701	40790.47	0.2198	40720.56	0.0481	3	132212	133410.01	0.9061	132442.17	0.1741
4	60170	60454.42	0.4727	60227.69	0.0959	4	158992	162451.91	2.1761	159378.98	0.2434
5	79806	80469.39	0.8313	79936.26	0.1632						
Shear Mode	81164	81394.24	0.2837	81205.98	0.0517						
6	99375	100660.20	1.2933	99622.29	0.2488						
7	118812	121018.92	1.8575	119231.42	0.3530						
8	138112	141594.19	2.5213	138767.63	0.4747						
9	157287	161048.88	2.3917	158253.67	0.6146						
10	176356	183660.76	4.1420	177716.66	0.7715						

In the Fig 3 , we can see the natural frequencies of the hinged-hinged beam for various values of the r factor using 70 elements.
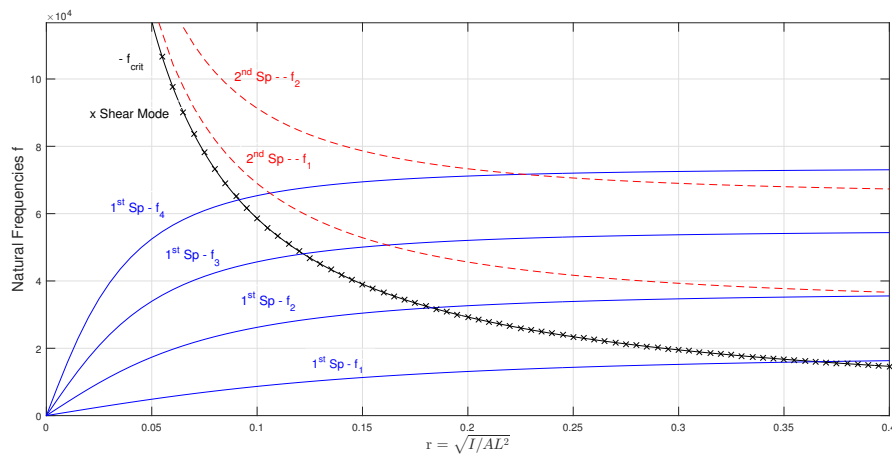

Figure 3: Frequency curves for the hinged-hinged Timoshenko beam (FEM - 70e)

Continuous curves represents first spectrum, the shear mode is the curve marked by "x" and the dashed curves represents second spectrum. Note that the shear mode frequency is not a boundary between the two frequency spectra. This also can be noticed for r factor equal to 0.25, which the shear mode curve is contained between two curves belonging to first spectrum. However, for each r factor, the natural frequencies from second spectrum are above shear mode frequencies. So, this spectrum appears only for higher frequencies than shear mode.

Mode shapes for the first ten frequencies of hinged-hinged beam are presented in the Fig. 4 for 70 element. In the Fig. 4-a and Fig.4-b showed the mode shapes before and after f_{crit}. In all examples the peak amplitude of the transverse deflection has been normalized to $0.02\,m$.
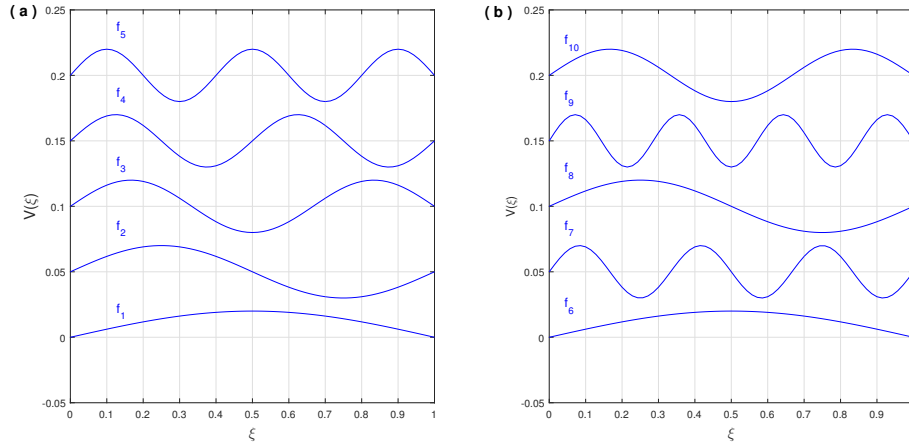
CILAMCE 2016

Proceedings of the *XXXVII Iberian Latin-American Congress on Computational Methods in Engineering*
Suzana Moreira Ávila (Editor), ABMEC, Brasília DF, Brazil, November 6-9, 2016

Figure 4: a) First five mode shapes for $f < f_{crit}$; b) First five mode shapes for $f > f_{crit}$

4.2 Slinding-slinding beam

Now, considering a sliding-sliding beam, first four natural frequencies for both frequency spectra are presented on Table 4. The second column represents the analytical results of TBT, and the third and fifth columns represent FEM results for 30 elements and 70 elements.

Table 4: Natural frequencies for the slinding-slinding Timoshenko beam (rad/s)

	1st Spectrum					2nd Spectrum				
Mode	TBT	FEM - 30e		FEM - 70e		Mode	TBT	FEM - 30e		FEM - 70e	
Number	Frequency	Frequency	Error (%)	Frequency	Error (%)	Number	Frequency	Frequency	Error (%)	Frequency	Error (%)
1	6712	6712.85	0.0127	6712.53	0.0079	1	89091	89420.32	0.3696	89151.54	0.0680
2	22137	22150.95	0.0630	22139.61	0.0118	2	108057	108691.89	0.5876	108174.10	0.1084
3	40705	40790.47	0.2100	40720.56	0.0382	3	132224	133410.01	0.8970	132442.17	0.1650
4	60177	60454.42	0.4610	60227.69	0.0842	4	159003	162451.91	2.1691	159378.98	0.2365

Frequency curves in function of dimensionless parameter r are shown in Fig. 5.
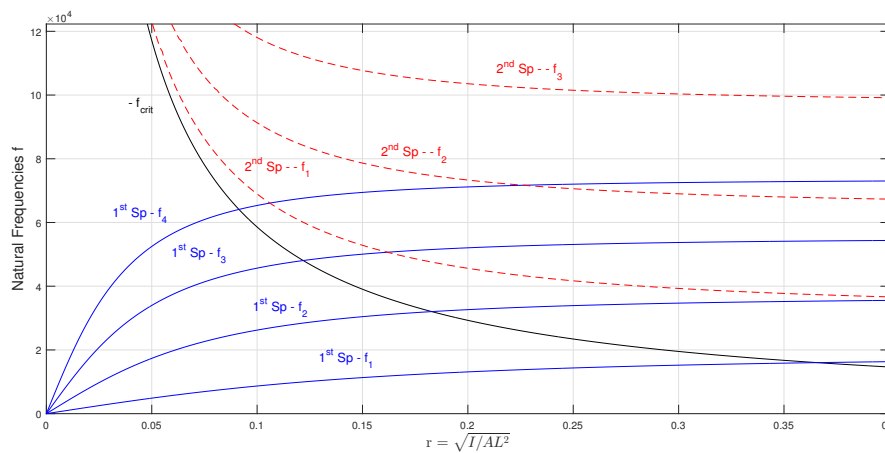
Figure 5: Frequency curves for the sliding-sliding Timoshenko beam (FEM - 70e)

Similarly to hinged-hinged frequency curves presented in Fig. 3, solid-lines are the first spectrum frequencies and dashed-lines corresponds to second spectrum frequencies. Observe that although sliding-sliding beam have double eigenvalues for frequencies beyond critical frequencies, there is no shear mode. Sliding-sliding beam have one rigid body mode. This rigid body mode is a translation of the rigid beam due to a constant force applied at the center of mass. The corresponding rigid body mode frequency is zero because the beam does not actually oscillate. Figure 6 presents the rigid body mode and the first ten mode shapes for a sliding-sliding beam. The rigid body mode have zero associated strain energy, and can be interpreted to mean the vibration occurs infinitely slowly, so there are zero associated inertia forces.
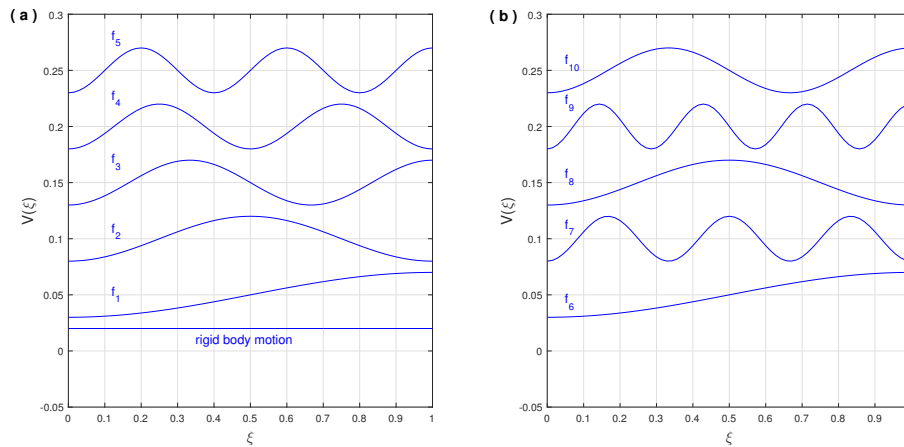
Figure 6: a) Rigid body and first five modes for $f < f_{crit}$; b) First five modes for $f > f_{crit}$ (FEM -70e)

4.3 Hinged-sliding beam

Han et al. (1999) discuss the relations between different boundary conditions by studying their symmetric and antisymmetric modes. It is observed that hinged-sliding is the symmetric mode of the hinged-hinged case and the antisymmetric mode of the sliding-sliding case.
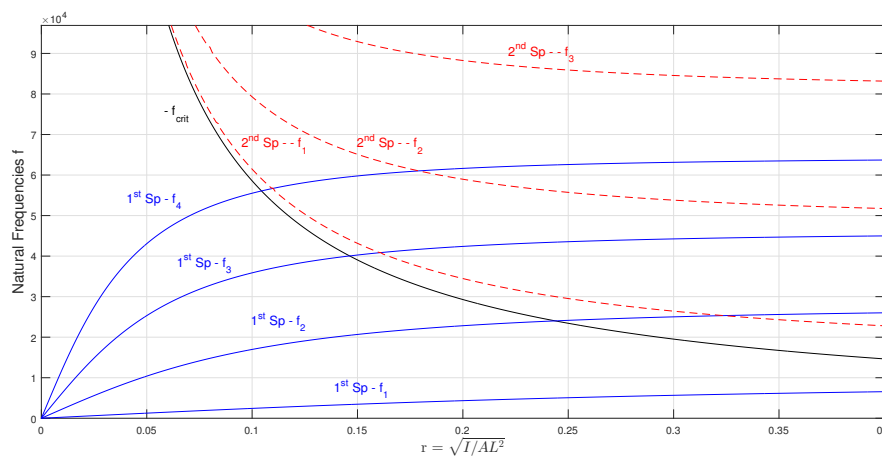

Figure 7: Frequency curves for the hinged-sliding Timoshenko beam (FEM - 70e)

Once the presence of second spectrum is confirmed on both previous cases, we investigate the phenomenon on hinged-sliding beam. The results obtained are presented in Fig. 7 and Fig. 8. Figure 7 shows that the presence of second spectrum (dashed-lines) is confirmed on hinged-sliding beam. However, unlike their symmetric (hinged-hinged) and antisymmetric (sliding-sliding) cases, hinged-sliding beam have no rigid body motion neither shear mode, as shown in Fig. 8.
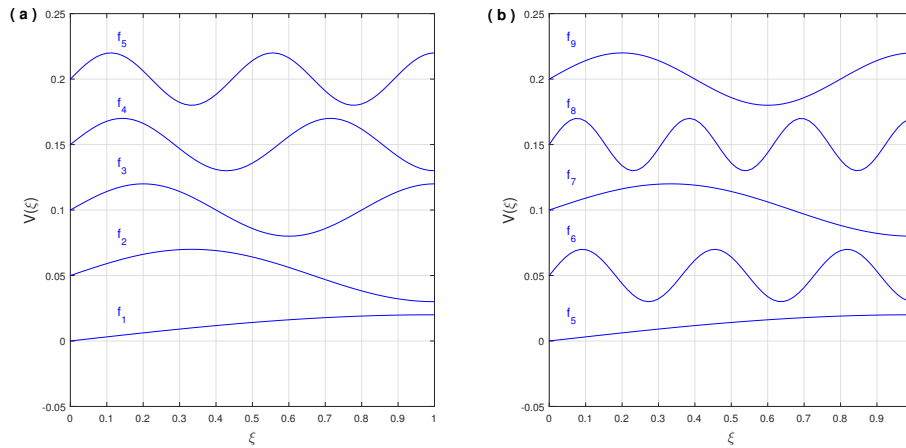

Figure 8: a) First five modes for $f < f_{crit}$; b) First five modes for $f > f_{crit}$ (FEM -70e)

4.4 Clamped-clamped beam

Consider a clamped-clamped beam, frequency curves are presented in Figs. 6 - 11 for both TBT and FEM with 10, 30 and 70 elements. Solutions of TBT frequency equation given in Table 1 are presented as a continuous functions of both r and s by solid-lines. FEM results are presented into dashed lines with different markers.
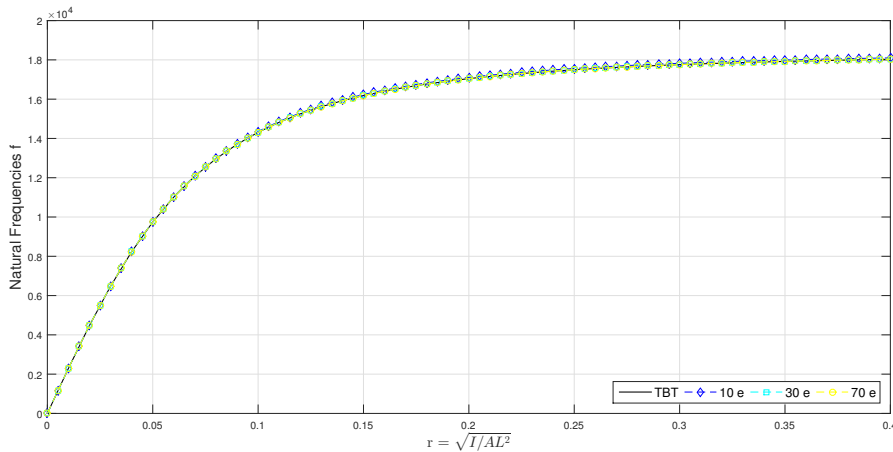

Figure 9: First frequency curves for the clamped-clamped Timoshenko beam

Figure 9 shown that finite element models provides well agreement with TBT first frequency curves for all three discretizations. However, as the mode increases only the 30 and 70 elements provides reasonable results.
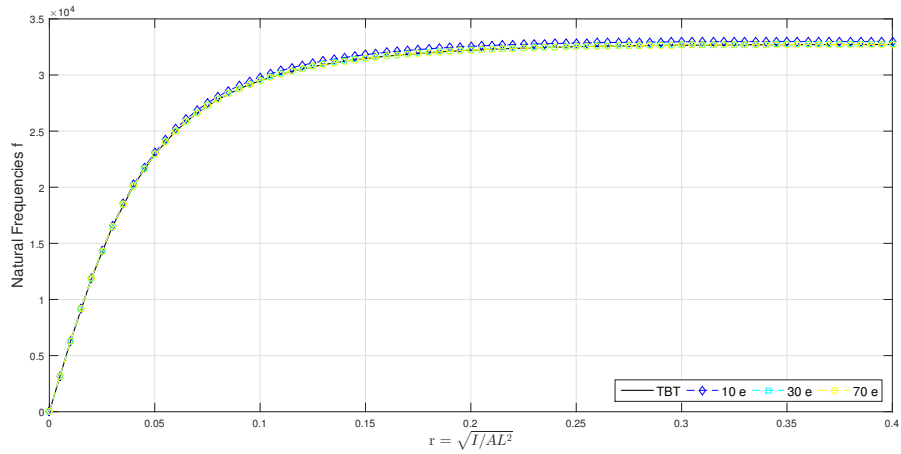
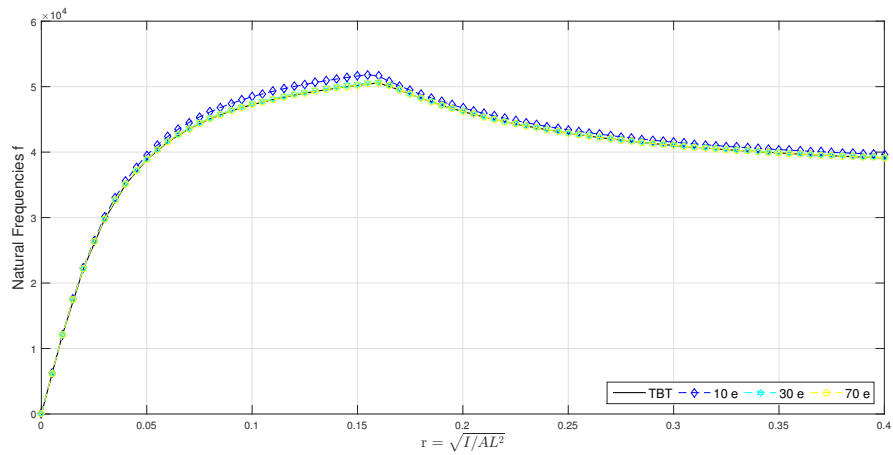**Figure 10: Second frequency curves for the clamped-clamped Timoshenko beam**

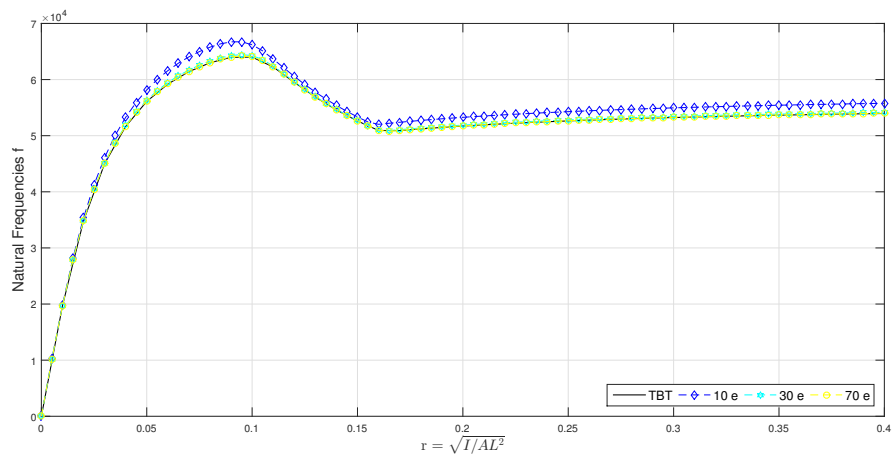**Figure 11: Third frequency curves for the clamped-clamped Timoshenko beam**

Figure 12: Fourth frequency curves for the clamped-clamped Timoshenko beam

CILAMCE 2016

Proceedings of the *XXXVII Iberian Latin-American Congress on Computational Methods in Engineering*
Suzana Moreira Ávila (Editor), ABMEC, Brasília DF, Brazil, November 6-9, 2016

It is observed in Fig. 10 that the 10 elements become less precise for values of dimensionless parameter r above 0.1, and that in Fig. 11 the precision of the results decreases for $r > 0.05$. Note that in Fig. 12 the precision of 30 and 70 elements still provide results accurately with TBT. Figure 13 presents the critical frequency f_{crit} and first six frequency curves for a 70 elements in order to demonstrate the frequency behavior to values above critical frequency.
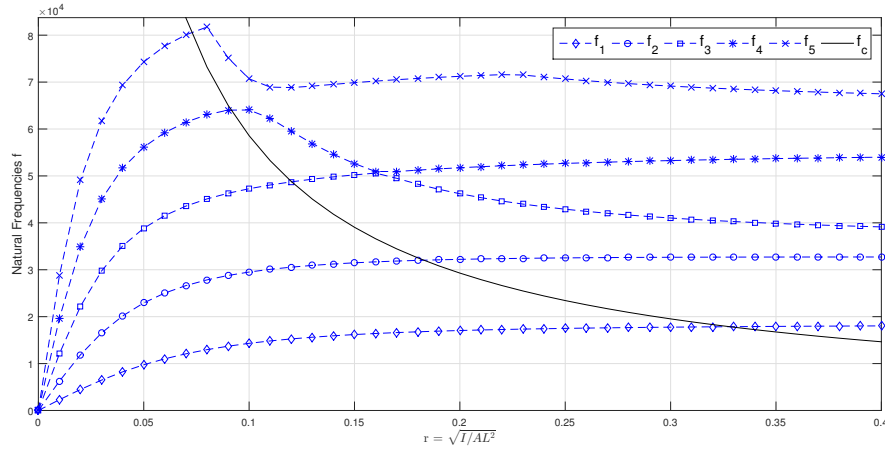

Figure 13: First six frequency curves for the clamped-clamped beam (FEM -70e)

Smith (2008) observed that TBT predicted that for $f < f_{crit}$ the number of peaks in the deflection profile increases by unit with increase in mode number, however, for $f > f_{crit}$, the number of peaks increases with each pair of modes. To illustrate clamped-clamped beam modes behavior we shown the first ten mode shapes on Fig. 14.
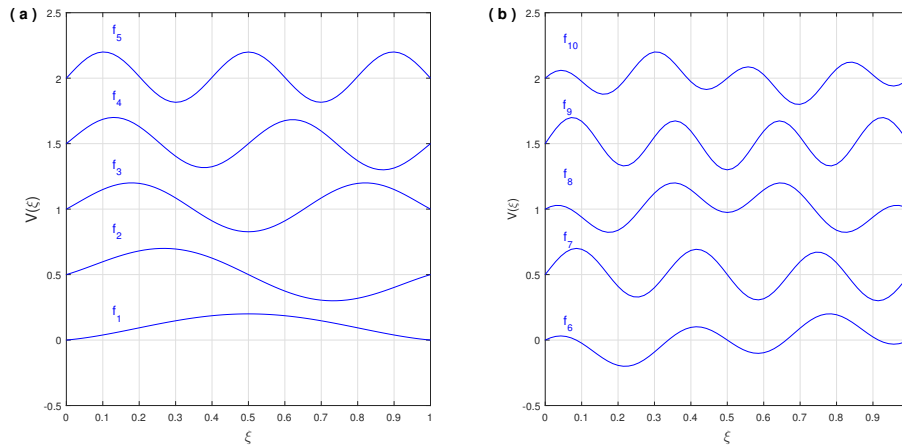

Figure 14: a) First five mode shapes for $f < f_{crit}$; b) First five mode shapes for $f > f_{crit}$ (FEM -70e)

5 Conclusion

In this paper, the full development and analysis of TBT for the transversely vibrating uniform beam were presented for classical boundary condition. Also, a review of classical Tim-

oshenko beam theory was presented. A finite element is developed in terms of dimensionless parameters of rotatory and shear based upon Hamilton's principle. Cubic and quadratic Lagrangian polynomials are used for total deflection and slope, respectively, where the polynomials are made interdependent by requiring them to satisfy both of the homogeneous and stationary TBT differential equations. Numerical examples are presented for four boundary conditions in order to study beam behavior above critical frequency. The investigation of mode shapes and frequency curves determined the existence of second spectrum in three boundary conditions: hinged-hinged, sliding-sliding and hinged-sliding, and the peculiar behavior on clamped-clamped beam where the number of peaks in the deflection increases by unit with each pair of modes. Finite elements results were in well agreement with other researchers results.

5.1   Permission

The authors are the only responsible for the printed material included in this paper.

REFERENCES

Anderson, R. A., 1953. Flexural vibration in uniform beams according to the Timoshenko theory. *Journal of Applied Mechanics*, vol. 20, pp. 504-510.

Archer, J. S., 1965. Consistent matrix formulations for structural analysis using finite element techniques. *AIAA Journal*, vol, 3, pp. 1910-1918.

Azevedo, A. C., Soares, A., & Hoefel, S. S., 2016. The second spectrum of Timoshenko beam. In *Proceedings of the IX Congresso Nacional de Engenharia Mecânica - CONEM 2016*, Fortaleza, Brazil.

Carnegie, W., Thomas, J., & Dokumci, E., 1969. An improved method of matrix displacement analysis in vibration problems. *Aeronautical Quarterly Journal*, vol. 20, pp. 321-332.

Cowper, G. R., 1966. The shear coefficient in Timoshenko's beam theory. *Journal of Applied Mechanics*, vol. 33, pp. 335-340.

Davis, R., Henshelland, R. D., & Warburton, G. B., 1972. A Timoshenko beam element. *Journal of Sound and Vibration*, vol. 22, pp. 475-487.

Dolph, C., 1954. On the Timoshenko theory of transverse beam vibrations. *Quarterly of Applied Mathematics*, vol. 12, pp. 175-187.

Dong, S. B., & Secor, G. A., 1973. Effect of transverse shear deformation on vibrations of planar structures composed of beam-type elements. *The Journal of the Acoustical Society of America*, vol. 53, pp. 12-127.

Downs, B., 1976. Vibration of a uniform, simply supported Timoshenko beam without transverse deflection. *Journal of Applied Mechanics*, vol. 43, pp. 671-674.

Egle, D. M., 1969. An approximate theory for transverse shear deformation and rotary inertia effects in vibrating beams. NASA-1317.

Euler, L., & Bousquet, M. M. C., 1744. Methodus inveniendi lineas curvas maximi minimive proprietate gaudentes, sive Solutio problematis isoperimetrici latissimo sensu accepti. *Apud Marcum-Michaelem Bousquet & Socios*

Friedman, Z., & Kosmatka, J. B., 1993. An improved two-node Timoshenko beam finite element. *Computers & Structures*, vol. 47, pp. 473-481.

Han, S. M., Benaroya, H., & Wei, T., 1999. Dynamics of transversely vibrating beams using four engineering theories. *Journal of Sound and Vibration*, vol. 225, pp. 935-988.

Huang, T. C., 1961. The effect of rotatory inertia and of shear deformation on the frequency and normal mode equations of uniform beams with simple end conditions. *Journal of Applied Mechanics*, vol. 28, pp. 579-584.

Hughes, T. J. R., Taylor, R. L., & Kanoknukulchoii, W., 1977. A simple and efficient plate element for bending. *International Journal for Numerical Methods in Engineering*, vol. 11, pp. 1529-1943.

Levinson, M., & Cooke, D. W., 1982. On the two frequency spectra of Timoshenko beams. *Journal of Sound and Vibration*, vol. 84, pp. 319-326.

McCalley, R. B., 1963. Rotary inertia correction for mass matrices. *General Electric Knolls Atomic Power Laboratory*, vol. Report DIG/SA, pp. 63-73.

Nickell, R. E., & Secor, G. A., 1972. Convergence of consistently derived Timoshenko beam finite elements. *International Journal for Numerical Methods in Engineering*, vol. 5, pp. 243-253.

Przemieniecki, J. S., 1968. Theory of matrix structural analysis.

Rayleigh, 1877. On progressive waves. In *Proceedings of the London Mathematical Society*, London, vol. IX, pp. 21-26.

Severn, R. T., 1970. Inclusion of shear deformation in the stiffness matrix for a beam element. *Strain Analysis*, vol. 5, pp. 239-241.

Smith, R. W. M., 2008. Graphical representation of Timoshenko beam modes for clamped-clamped boundary conditions at high frequency: Beyond transverse deflection. *Wave Motion*, vol. 45, pp. 785-794.

Soares, A., & Hoefel, S. S., 2015. Modal analysis for free vibration of four beam theories. In *Proceedings of the 23rd International Congress of Mechanical Engineering - COBEM 2015*, Rio de Janeiro, Brazil.

Tessler, A., & Dong, S. B., 1981. On a hierarchy of conforming Timoshenko beam elements. *Computers and Structures*, vol. 14, pp. 335-344.

Thomas, D. L., Wilson, J. M. W., & Wilson, R. R., 1973. Timoshenko beam finite elements. *Journal of Sound and Vibration*, vol. 31, pp. 315-330.

Thomas, J., & Abbas,B. A. H., 1975. Finite element model for dynamic analysis of Timoshenko beam. *Journal of Sound and Vibration*, vol. 41, pp. 291-299.

Timoshenko, S. P., 1921. On the correction for shear of the differential equation for transverse vibration of prismatic bars. *Philosophical Magazine*, vol. 41, pp. 744-746.

Traill-Nash, R. W., & Collar, A. R., 1953. The effects of shear flexibility and rotatory inertia on bending vibrations beams. *Quaterly Journal of Mechanics and Applied Mathematics*, vol. 6, pp. 186-213.